ANULEWICZ, R., KRYGOWSKI, T. M. & PNIEWSKA, B. (1990). *Acta Cryst.* C**46**, 2121–2123.
BRAUN, U., RICHTER, R., SIELER, J. & BEYER, L. (1988). *Acta Cryst.* C**44**, 355–357.
CISZAK, E., GDANIEC, M., JASKÓLSKI, M. & KOSTURKIEWICZ, Z. (1988). *Acta Cryst.* C**44**, 2144–2146.
CISZAK, E., GDANIEC, M., JASKÓLSKI, M., KOSTURKIEWICZ, Z., OWSIAŃSKI, J. & TYKARSKA, E. (1989). *Acta Cryst.* C**45**, 433–438.
CISZAK, E., GDANIEC, M. & KOSTURKIEWICZ, Z. (1987). *Acta Cryst.* C**43**, 1362–1364.
CISZAK, E., JASKÓLSKI, M. & KOSTURKIEWICZ, Z. (1990). *Acta Cryst.* C**46**, 456–458.
EXNER, O., BUDESINSKY, M., HYNK, D., VESETECKA, V. & RACZYŃSKA, D. (1988). *J. Mol. Struct.* **178**, 147–159.
GILLI, G. & BERTOLASI, V. (1979). *J. Am. Chem. Soc.* **101**, 7704–7711.
IVASAKI, F. & AKIBA, K. (1981). *Acta Cryst.* B**37**, 185–187.
KNYCHAŁA, A., RYCHLEWSKA, U., KOSTURKIEWICZ, Z. & OSZCZAPOWICZ, J. (1989). *Acta Cryst.* C**45**, 1647–1649.
KRAJEWSKI, J., URBAŃCZYK-LIPKOWSKA, Z., GLUZIŃSKI, P., BUŚKO-OSZCZAPOWICZ, J., OSZCZAPOWICZ, J., BLEIDELIS, J. & KEMME, A. (1981). *Pol. J. Chem.* **55**, 1015–1024.
NORRESTAM, R., MERTZ, S. & CROSSLAND, I. (1983). *Acta Cryst.* C**39**, 1554–1556.
OSZCZAPOWICZ, J., TYKARSKA, E., JASKÓLSKI, M. & KOSTURKIEWICZ, Z. (1986). *Acta Cryst.* C**43**, 1816–1818.
SOHAR, P. (1967). *Acta Chim. Acad. Sci. Hung.* **54**, 91–97.
SURMA, K., JASKÓLSKI, M., KOSTURKIEWICZ, Z. & OSZCZAPOWICZ, J. (1988). *Acta Cryst.* C**44**, 1031–1033.
TINANT, B., DUPONT-FENEAU, J., DECLERCQ, J.-P., PODLAHA, J. & EXNER, O. (1989). *Collect. Czech. Chem. Commun.* **54**, 3245–3252.
TYKARSKA, E., JASKÓLSKI, M. & KOSTURKIEWICZ, Z. (1986*a*). *Acta Cryst.* C**42**, 208–210.
TYKARSKA, E., JASKÓLSKI, M. & KOSTURKIEWICZ, Z. (1986*b*). *Acta Cryst.* C**42**, 740–743.
TYKARSKA, E. & KOSTURKIEWICZ, Z. (1991). *Pol. J. Chem.* Accepted.
WINKLER, F. K. & DUNITZ, J. D. (1971). *J. Mol. Biol.* **59**, 169–182.

*Acta Cryst.* (1992). B**48**, 476–488

# Structure of a Pepsin/Renin Inhibitor Complex Reveals a Novel Crystal Packing Induced by Minor Chemical Alterations in the Inhibitor

BY LIQING CHEN,* JOHN W. ERICKSON,† TIMOTHY J. RYDEL,‡ CHANG H. PARK, DAVID NEIDHART,§ JAY LULY¶ AND CELE ABAD-ZAPATERO**

*Laboratory of Protein Crystallography, D-46Y, AP-9A, and Cardiovascular Chemistry, D-47L, Abbott Laboratories, Abbott Park, IL* 60064, *USA*

(*Received* 23 *September* 1991; *accepted* 10 *February* 1992)

## Abstract

The structure determination by molecular replacement methods of a monoclinic pepsin/renin inhibitor complex crystal, with two molecules in the asymmetric unit, is presented. The atomic model, consisting of two liganded pepsin molecules and 110 water molecules, has been refined to a final crystallographic $R$ value of 0.139 for data between 8 and 2.9 Å resolution. The structure reveals a previously undescribed pepsin dimer formed predominantly by polar interactions. Inhibitor binding induces global structural changes in the native enzyme similar, but not identical, to the ones observed in other chemically similar pepsin/renin inhibitor complexes crystallized in an orthorhombic form. A region of the polypeptide chain (residues 292–297) which was not visible in the orthorhombic crystal is well ordered in the presently described structure; possibly induced by crystal contacts. The crystal packing of native pepsin is compared with the two different crystal forms of the inhibited enzyme.

## Introduction

Pepsin belongs to the class of enzymes known as aspartic proteinases. Members of this class are widespread in nature and are responsible for a myriad of important commercial and biomedical processes (Kostka, 1985; Davies, 1990). Renin is a particularly interesting example of the group because of its role in the first, and limiting, step of the angiotensin–angiotensinogen cascade, which regulates hypertension in higher organisms. Highly purified renin from mammalian or recombinant sources has been difficult to obtain in large quantities and therefore porcine

* Present address: Department of Biology, Room 16-739, Massachusetts Institute of Technology, 77 Massachusetts Avenue, Cambridge, MA 02139, USA.
† Present address: NCI, Frederick Cancer Research and Development Center, PO Box B, Frederick, MD 21701, USA.
‡ Present address: Research and Development, Miami Valley Laboratories, The Procter and Gamble Company, PO Box 398707, Cincinnati, OH 45239-8707, USA.
§ Present address: Monsanto Corporate Research, BB4K, 700 Chesterfield Village Parkway, Chesterfield, MO 63198, USA.
¶ Cardiovascular Chemistry, D-47L.
** To whom correspondence should be addressed.

0108-7681/92/040476-13$06.00 

pepsin has been used as a valuable model for the design of drugs controlling hypertension because of the high sequence identity (39%) (Sham, Bolis, Stein, Fesik, Marcotte, Plattner, Rempel & Greer, 1988; Bolis & Greer, 1989; Hutchins & Greer, 1991).

Crystallographic studies of pepsin and several fungal enzymes of this class (Andreeva, Fedorov, Gustchina, Riskulov, Safro & Shutzkever, 1978; Hsu, Delbaere, James & Hofmann, 1977; James & Sielecki, 1983; Suguna, Bott, Padlan, Subramanian, Sheriff, Cohen & Davies, 1987; Blundell, Jenkins, Pearl, Sewell, Cooper, Tickle, Veerapandian & Wood, 1990) established the fold of the approximately 330-residue polypeptide. It revealed a bilobal structure containing an approximate intramolecular dyad comprising a core of approximately 70 residue pairs with an r.m.s. deviation of 2.4 Å (Abad-Zapatero, Rydel & Erickson, 1990; Sielecki, Fedorov, Boodhoo, Andreeva & James, 1990). Each core contributes an essential aspartic acid residue to the catalytic site implying that the eukaryotic aspartic proteinases evolved by gene duplication of a primordial gene (Tang, James, Hsu, Jenkins & Blundell, 1978). This hypothesis has received further support by the structural characterization of two retroviral proteases which exist as dimers of identical subunits of approximately 100 residues each (Miller, Jaskolski, Rao, Leis & Wlodawer, 1989; Navia, Fitzgerald, McKeever, Leu, Heimbach, Herber, Sigal, Darke & Springer, 1989; Wlodawer, Miller, Jaskolski, Sathyanarayana, Baldwin, Weber, Selk, Clawson, Schneider & Kent, 1989) and which are structurally closely related to the larger monomeric enzymes (Rao, Erickson & Wlodawer, 1991). An intradomain pseudodyad was also found (Blundell, Sewell & McLachlan, 1979; Andreeva & Gustchina, 1979) within each lobe, relating 26 equivalent $C_\alpha$ pairs in the amino domain with an r.m.s. deviation of 2.4 Å, but only 23 pairs (r.m.s. 2.7 Å) at the carboxy end (Abad-Zapatero, Rydel & Erickson, 1990).

During the last decade a great deal of effort has been directed to the design of renin inhibitors based on the knowledge obtained from the comparative modeling of aspartic proteinases and from the crystallographic analysis of several enzyme/inhibitor complexes, using the known structure of the fungal enzymes (Hutchins & Greer, 1991). No crystal structure of a renin/inhibitor complex has yet been reported. However several high-resolution crystal structures of endothia pepsin/renin inhibitor complexes have been determined (Blundell, Cooper, Foundling, Jones, Atrash & Szelke, 1987; Foundling, Cooper, Watson, Cleasby, Pearl, Sibanda, Hemmings, Wood, Blundell, Valler, Norey, Kay, Boger, Dunn, Leckie, Jones, Atrash, Hallett & Szelke, 1987; Sali, Veerapandian, Cooper, Foundling, Hoover & Blundell, 1989; Veerapandian, Cooper, Sali & Blundell, 1990). More recently the structure of an orthorhombic crystal form of pepsin/renin inhibitor complexes has been determined and refined to 1.8 Å resolution (Abad-Zapatero, Rydel, Neidhart, Luly & Erickson, 1992).

An extensive analysis of the mode of binding of renin inhibitors to pepsin has been hindered by the existence of two separate crystal forms (Table 1). One form is orthorhombic ($P2_12_12_1$) with cell constants $a = 124.0$, $b = 65.0$ and $c = 36.2$ Å and one molecule of the pepsin/inhibitor complex in the asymmetric unit. Two structures of this class have been reported recently (Abad-Zapatero, Rydel, Neidhart, Luly & Erickson, 1992) allowing an initial analysis of the mode of inhibitor binding and of the conformational changes induced by ligand. A monoclinic crystal form ($P2_1$, unique axis $c$, $a = 54.0$, $b = 74.3$, $c = 76.7$ Å, $\gamma = 100.8°$) with two molecules in the asymmetric unit was obtained almost simultaneously, using similar crystallization conditions with inhibitors lacking an iodine at the $P_3$ position (Table 1, Fig. 1).

This paper presents the structure determination of a pepsin/A62095 complex in the second crystal form by molecular replacement methods (Rossmann, 1972). The structural alterations induced in the native protein by inhibitor binding are discussed and compared with the rearrangements observed in the orthorhombic pepsin/inhibitor complex. A brief discussion of the inhibitor binding is presented and the noncrystallographic dimer which forms the basic building unit of the crystal is described. The crystal packings of the two different crystal forms found in pepsin/inhibitor complexes are compared with each other as well as with native pepsin.

## Materials and methods

### *Crystallization*

Porcine pepsin was obtained from Sigma Chemical Co. and prepared as described previously (Abad-Zapatero, Rydel & Erickson, 1990). Crystals of the enzyme/inhibitor complex were obtained by a small modification of the protocol used to grow crystals of the native enzyme (Andreeva, Zdanov, Gustchina & Fedorov, 1984; Abad-Zapatero, Rydel & Erickson, 1990). The enzyme was dissolved in distilled water at approximately 20 mg ml$^{-1}$, adjusted to pH 2.0, and ethanol added to a concentration near 20% (*v*/*v*: ethanol/water). A concentrated ethanol solution of the inhibitor A62095 (Fig. 1) was added to achieve a stoichiometric enzyme/inhibitor ratio slightly over 1:1. The crystals grew in a few days as prismatic rods, frequently aggregated. They were characterized by precession photography as monoclinic, with cell

Table 1. *Crystal data of pepsin and its complexes with renin inhibitors*

| | Pepsin | + A62095* | + A61963* | + A63218* | + A66702* |
|---|---|---|---|---|---|
| Space group | $P2_1$ | $P2_1$ | $P2_1$ | $P2_12_12_1$ | $P2_12_12_1$ |
| $a$ (Å) | 55.2 | 54.1 | 54.1 | 123.9 | 124.0 |
| $b$ (Å) | 73.6 | 74.4 | 74.4 | 64.9 | 65.0 |
| $c$ (Å) | 36.4 | 76.5 | 76.7 | 36.2 | 36.2 |
| $\gamma$ (°) | 104.0 | 100.8 | 100.8 | | |
| Volume (Å$^3$) | 143 500 | 302 500 | 303 250 | 291 100 | 291 800 |
| Solvent content (%) | 42 | 46 | 46 | 41 | 41 |
| $Z$ | 2 | 4 | 4 | 4 | 4 |
| Asymmetric unit | Monomer | Dimer | Dimer | Monomer | Monomer |
| Resolution (Å) | 2.3† | 2.9† | 2.9† | 2.2 | 1.8 |

* The structures corresponding to these compound numbers are presented in Fig. 1.
† Available data, not limit of diffraction pattern.

constants $a = 54.0$, $b = 74.3$, $c = 76.7$ Å and $\gamma = 100.8°$ ($c$ axis unique) and diffracting to at least 2.9 Å. The volume of the unit cell was essentially double that of the unit cell of the monoclinic native pepsin (Table 1), and therefore strongly suggested the presence of two pepsin/inhibitor complexes per asymmetric unit.

*Data collection and processing*

Data were collected using a Rigaku AFC-5 diffractometer, equipped with a graphite crystal monochromator and evacuated tunnel to reduce air scattering. A Rigaku RU-200 rotating anode, operated at 50 kV and 80 mA, was used as the X-ray source. Data were collected using the $\omega$-scan technique as described for the crystals of native pepsin (Abad-Zapatero, Rydel & Erickson, 1990). Background-corrected intensities were reduced to structure factors after applying Lorentz and polarization corrections as implemented by the integrated data-collection software *TEXSAN* (Molecular Structure Corporation, 1989). Crystal decay was monitored by measuring a set of seven reflections throughout the course of data collection at regular intervals, typically after a block of 300 reflections. Decay was computed as a function of both time and resolution by fitting the structure factors to a linear function of time, multiplied by an exponential decay curve. Maximum observed decay ranged from 10 to 25% for the low- and high-resolution standard reflections, respectively. The decay correction was computed from the least-squares-fitted equation and applied to each reflection. An absorption correction was applied after fitting a symmetrical curve to the $\psi$-scan measurements. Further data processing was carried out using the program *PROTEIN* (Steigemann, 1974).

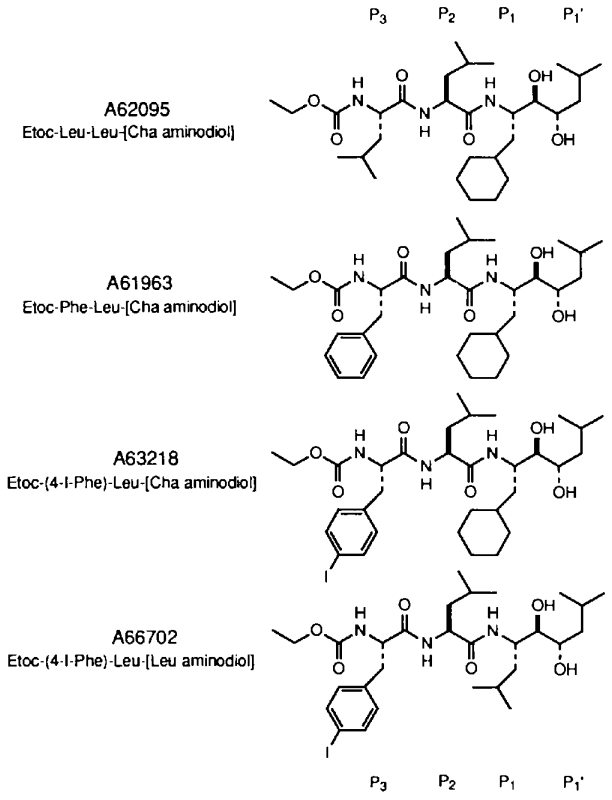


Fig. 1. Schematic representation of the structure of several renin inhibitors co-crystallized with porcine pepsin. The lattice cell parameters for the crystals of the different complexes are presented in Table 1.

Crystals were soaked in 1 and 10 m$M$ $HgCl_4^{2-}$ for 7 days in attempts to prepare heavy atoms similar to the ones used in the original structure solution of pepsin (Andreeva, Zdanov, Gustchina & Fedorov, 1984). The lower concentration soak did not exhibit any isomorphous changes and the high-concentration mercury derivative showed weak differences but the difference Patterson was not interpretable.

An initial 3 Å data set was collected from a thin (0.4 × 0.4 × 0.15 mm) crystal consisting of 13 550 measurements which was reduced to only 7302 ($F > 3\sigma$) independent reflections because of severe radiation damage. Data were also collected from a larger crystal (0.5 × 0.5 × 0.3 mm) soaked in 1 m$M$ $HgCl_4^{2-}$ for 7 days. A total of 13 404 reflections were collected which reduced to 11 751 (97% of theoretically possible to 3 Å resolution) reflections

with an internal agreement of 5.4% for 926 symmetry-equivalent reflections. Scaling of this putative $HgCl_4^{2-}$ derivative to native showed that there had been no substitution and therefore these data were considered as native and merged in the final native data set. The 2.9 Å resolution data set was recollected from a freshly grown complex crystal (0.3 × 0.4 × 0.4 mm) starting from the high-resolution shell and progressing towards the lower resolution. This set consisted of 13 460 observations which reduced to 12 353 unqiue reflections with an $R_{sym} = 3.4\%$.

Merging of these three sets together showed that the best joint data set was obtained by merging only sets 2 and 3 to include 24 379 observations for 11 951 unique reflections with an $R_{merge} = 4.4\%$. This set comprised 11 951 reflections out of 13 736 possible (87%) within the 2.9 Å resolution sphere (95% complete to 3 Å resolution). This set was used in the structure solution by molecular replacement.

*Structure determination*

The rotation and translation function searches were performed using the program packages *MERLOT* (Fitzgerald, 1988) and *ROTRAN* (Craven, 1975). The self-rotation function had two peaks: (i) a broad peak at the $\kappa = 40°$ section, approximately parallel to the crystallographic *b* axis (Fig. 2*a*); (ii) another, very sharp peak in the $\kappa = 180°$ section, on a plane perpendicular to the *b* axis and inclined 19.4° with respect to the crystal *c* axis (Fig. 2*b*). These two peaks are related by the crystallographic $2_1$ screw along *c* and either of them, independently, confirmed the presence of two pepsin molecules in the asymmetric unit.

The search model consisted of all atoms of the well-refined pepsin/A66702 complex ($R = 0.170$ at 1.8 Å resolution; Abad-Zapatero, Rydel, Neidhart,

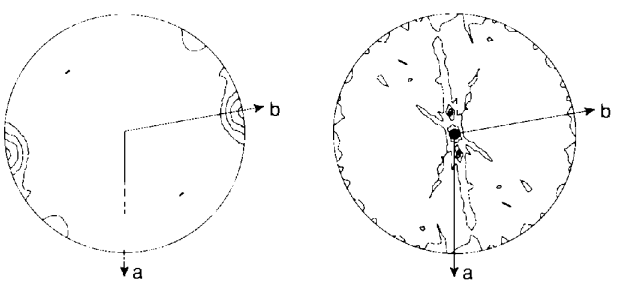


(*a*) (*b*)

Fig. 2. Stereographic projection of the best self-rotation function results for the pepsin/A62095 complex obtained using an integration radius of 30 Å and resolution limits between 8 and 4 Å. (*a*) $\kappa = 40°$, (*b*) $\kappa = 180°$. The origin peak, along the crystallographic *c* axis ($\kappa = 180°$, $\varphi = 0°$) in (*b*), is 50. Solid line contours are drawn at intervals corresponding to 10% of the origin.

Table 2. *Cross-rotation function results for search model* (I)

(*a*) Resolution limits: 8–5 Å; integration radius: 29.0 Å

| Peak rank | α (°) | β (°) | γ (°) | Height |
|---|---|---|---|---|
| 1 | 142.50 | 50.00 | 145.00 | 100.0 (8.1σ) |
| 2 | 42.50 | 160.00 | 5.00 | 79.0 (6.4σ) |
| 3 | 37.50 | 160.00 | 0.00 | 77.8 (6.3σ) |
| 4 | 47.50 | 160.00 | 10.00 | 77.1 (6.2σ) |
| 5 | 32.50 | 160.00 | 355.00 | 73.0 (5.9σ) |
| 6 | 144.45 | 84.47 | 126.51 | 71.2 (5.7σ) |
| 7 | 142.23 | 61.55 | 131.87 | 69.7 (5.6σ) |
| 8 | 57.50 | 160.00 | 20.00 | 67.6 (5.4σ) |
| 9 | 27.50 | 140.00 | 335.00 | 65.3 (5.3σ) |

(*b*) Resolution limits: 8–4 Å; integration radius: 23.0 Å

| Peak rank | α (°) | β (°) | γ (°) | Height |
|---|---|---|---|---|
| 1 | 137.50 | 50.00 | 150.00 | 100.0 (6.3σ) |
| 2 | 145.75 | 86.14 | 126.59 | 81.8 (5.1σ) |
| 3 | 115.00 | 155.00 | 115.00 | 70.0 (4.4σ) |
| 4 | 24.71 | 95.41 | 19.42 | 69.5 (4.4σ) |

Table 3. *Cross-rotation function results for search model* (II)

Resolution limits: 8–4 Å; integration radius: 23.0 Å.

| Peak rank | α (°) | β (°) | γ (°) | Height |
|---|---|---|---|---|
| 1–72 | 0.00 | 0.00 | 0.00 | 100.0 (6.0σ) |
| 73 | 175.00 | 40.00 | 185.00 | 79.6 (4.8σ) |
| 74 | 0.00 | 40.00 | 180.00 | 67.0 (4.0σ) |
| 75–79 | 60.00 | 175.00 | 255.00 | 67.0 (4.0σ) |
| 80 | 80.00 | 45.00 | 85.00 | 66.4 (4.0σ) |

Luly & Erickson, 1992) except the iodo-Phe side chain of A66702 (Leu in A62095, Table 1). It was placed in an arbitrary 160 × 160 × 160 Å *P*1 orthogonal unit cell and structure factors were calculated to 3.5 Å resolution. The Euler angle search ranges for cross-rotation peaks were α 0 to 180, β 0 to 180, γ 0 to 360° using a coarse grid of 5.0°, a radius of integration of 29 Å and resolution limits between 8 and 5 Å. The highest peak (8.1σ) was found at $\alpha = 142.5$, $\beta = 50.0$ and $\gamma = 145.0°$, and was considered to be the solution for one (molecule *A*) of the two molecules in the asymmetric unit. However, at this resolution the solution for the second molecule (*B*) was ambiguous. The first two peaks in Table 2(*a*) were considered a tentative solution for the orientation of the two independent molecules and their values refined using the Lattman rotation function (Lattman & Love, 1972).

The translation function of Crowther & Blow (1967) was used to determine the translational components along the three axes for the two unknown molecules in the $P2_1$ unit cell. The translation function results gave a distinct peak (6.2σ) in the Harker section corresponding to the *A*–*A*′ intermolecular vector for resolution ranges between 8 and 5 Å. However, the solution for molecule *B* was uncertain since the *B*′–*B* vector search results were noisy, varied with resolution and no distinct peak was found to correlate with the cross (*A*–*B*) vector search.

Table 4. *Translation-function results*

Resolution limits: 8–5 Å; orientation of molecule *A*: $\alpha = 0.0$, $\beta = 0.0$, $\gamma = 0.0°$; orientation of molecule *B*: $\alpha = 175.0$, $\beta = 40.0$, $\gamma = 185.0°$.

| | Peak | $\Delta x$ | $\Delta y$ | $\Delta z$ | Height | $x$ | $y$ | $z$ |
|---|---|---|---|---|---|---|---|---|
| *A′ A* | 1 | 0.00 | 0.00 | 50.00 | 100.0 (6.0$\sigma$) | 0.00 | 0.00 | *A* |
| *B′ B* | 1 | 72.00 | 80.00 | 50.00 | 100.0 (6.5$\sigma$) | 0.36 | 0.40 | *B* |
| | | | | | | $x_A - x_B$ | $y_A - y_B$ | $z_A - z_B$ |
| *B–A* | 1 | 14.82 | 61.28 | 78.36 | 100.0 (9.1$\sigma$) | 0.36 | 0.40 | 0.78 |

Table 5. *Rigid-body refinement of the molecular replacement solution*

Final rotation and translation solutions

| Molecule | $\alpha$ ( ) | $\beta$ ( ) | $\gamma$ ( ) | $x$ | $y$ | $z$ |
|---|---|---|---|---|---|---|
| *A* | 0.0 | 0.0 | 0.0 | 0.005 | 0.0 | 0.0 |
| *B* | 175.5 | 39.5 | 184.5 | 0.8518 | 0.3922 | 0.2164 |

Rigid-body refinement

Resolution limits: 8–2.9 Å; r.m.s. positional shifts: 0.62 Å; $R_{start} = 0.407$; $R_{end} = 0.336$.

| Group | $\alpha$ ( ) | $\beta$ ( ) | $\gamma$ ( ) | $\Delta x$ (Å) | $\Delta y$ (Å) | $\Delta z$ (Å) |
|---|---|---|---|---|---|---|
| Pepsin *A* | −0.16 | −0.19 | 0.79 | −0.13 | 0.46 | −0.05 |
| Pepsin *B* | −0.49 | 0.91 | −2.05 | −0.04 | 0.44 | −0.03 |
| Inhibitor *A* | 0.03 | 0.03 | 0.01 | −0.39 | 0.72 | 0.05 |
| Inhibitor *B* | 0.00 | 0.01 | −0.05 | 0.50 | 0.87 | 0.02 |

The initial model was rotated and translated to the solution of molecule *A* and used as a new search model (model II) for the following rotation and translation searches under the same conditions as the original model (8–5 Å; 29 Å). The results also failed to locate molecule *B*. The cross-rotation function was calculated again using 8–4 Å as resolution limits and 23 Å for integration radius. A distinct (4.8$\sigma$) second highest peak (No. 73, Table 3) was found that had an angular relationship with molecule *A* matching the self-rotation peak at $\varphi = 90$, $\psi = 90$ and $\kappa = 40°$ (Fig. 2*a*, $\varphi$ angle starts at $a^*$ axis). The peak was assigned as the orientation of molecule *B* and a translation function search based on the new rotation solution unambiguously found the consistent molecular translations (Table 4) with only one peak being present in each of the three vector searches. The rotation and translation solutions for the two molecules were refined by the *R*-factor minimization to an *R* factor of 0.43 (8–5 Å). The final orientations and positions of the two independent molecules are listed in Table 5. A check on the packing of the two molecules in the crystal revealed no bad intermolecular contacts.

In retrospect, our difficulties in obtaining distinct solutions for the orientation and position of the second molecule could have been avoided by including the higher-resolution data in the initial cross-rotation searches (Cygler & Anderson, 1988*a*,*b*; Sheriff, Padlan, Cohen & Davies, 1990). After the structure was determined, the correct orientations for molecules *A* and *B* were obtained from the cross-rotation function calculated with an integration radius of 23 Å and resolution limits of 8 and 4 Å. The peak corresponding to the second molecule (*B*) (Table 2*b*) is essentially equivalent to peak 6 in the original cross-rotation function (Table 2*a*).

*Refinement*

The refinement of the molecular replacement model was carried out at 8–2.9 Å resolution using the program package *XPLOR* (Brünger, Karplus & Petsko, 1989). First, the two separate protein molecules and the two associated inhibitor molecules were refined as rigid bodies reducing the *R* factor from 0.407 to 0.336 (Table 5). Excluding the inhibitors, the two polypeptide chains were then refined by a total of 160 cycles of conjugate gradient energy minimization without simulated annealing since the starting pepsin model from the pepsin/A66702 complex had been well refined at 1.8 Å resolution (Abad-Zapatero, Rydel, Neidhart, Luly & Erickson, 1992). Both the $2F_o - F_c$ and $F_o - F_c$ maps calculated after the refinement showed the electron density clearly for the two A62095 inhibitors. The maps also revealed that a loop region (residues 292–297) needed to be rebuilt (Fig. 3). This loop was not well characterized, either in the orthorhombic crystal form, or in the native pepsin (Abad-Zapatero, Rydel & Erickson, 1990) because of disorder, but in the current structure it had a well defined electron density associated with it. After fitting the inhibitors and rebuilding the loop, a few other minor adjustments were performed and the resulting model was refined again by energy minimization to an *R* factor of 0.173. Twenty cycles of restrained individual isotropic *B* factor refinement brought the *R* factor further down to 0.162. At this stage well ordered water molecules were located from the difference Fourier map ($F_o - F_c$) and added as O

atoms to the model only if they had a peak height over $3\sigma$ in the difference density map and formed hydrogen bonds with protein atoms. A total of 110 water molecules were found in this way. A final round of refinement completed the structure determination with an $R$ factor of 0.139 (8–2.9 Å) and r.m.s. deviations from ideal bond lengths and angles of 0.014 Å and 3.17°, respectively (Table 6).*

## Results and discussion

### *Overall structure*

Two crystallographically independent molecules (*A* and *B*) of the pepsin/A62095 complex are obtained from the structure determination of this monoclinic crystal form. There are no contacts (<4.1 Å) between them. Nonetheless, by the crystallographic symmetry acting on *B*, two molecules (*A* and *B'*) are closely associated *via* a 180° rotation and a small translation with axial components (1.04, 0.34, −0.40 Å) (Fig. 9). The rotation axis is inclined 19.4° with respect to the crystal *c* axis forming a noncrystallographic dimer. A total of 15 direct protein–protein hydrogen bonds participate in the association (Table 7) and a total of 110 putative water molecules have been positioned associated with the dimer. Pepsin/inhibitor complexes which crystallize in the orthorhombic space group (Table 1) do not have noncrystallographic symmetry and exhibit a different packing arrangement (see below). To our knowledge, native pepsin is not known to dimerize, although an aspartic proteinase from *C. albicans* has been reported to form dimers under alkaline conditions and in the presence of pepstatin (Rüchel, 1981).

* A complete set of atomic coordinates for the two independent pepsin/A62095 complexes in the asymmetric unit and the observed structure factors have been deposited with the Protein Data Bank, Brookhaven National Laboratory (Reference: 1PSA, R1PSASF), and are available in machine-readable form from the Protein Data Bank at Brookhaven. The data have also been deposited with the British Library Document Supply Centre as Supplementary Publication No. SUP 37063 (as microfiche). Free copies may be obtained through The Technical Editor, International Union of Crystallography, 5 Abbey Square, Chester CH1 2HU, England.

Fig. 3. Stereo diagram of the portion of the polypeptide chain near the loop 292–297. Thick lines depict the refined model for this part of the pepsin structure. Thin lines represent the conformation of the same loop in the native pepsin structure [Protein Data Bank set 4PEP; Sielecki, Fedorov, Boodhoo, Andreeva & James (1990)]. The thin $C_\alpha$ tracing corresponds to the path of the chain assumed in the pepsin/A66702 complex where this region of the polypeptide chain was considered to be disordered.

Table 6. *Final statistics for the refinement of the pepsin/A62095 complex*

| | |
|---|---|
| *R* factor | 0.139 |
| Resolution (Å) | 8–2.9 |
| Reflections | 11 284 |
| Non-H protein atoms | 4858 |
| Non-H inhibitor atoms | 76 |
| Water molecules | 110 |
| R.m.s. deviations from ideality | |
| Bond lengths (Å) | 0.014 |
| Bond angles (°) | 3.2 |
| Dihedral angles (°) | 27.6 |
| Improper dihedral angles (°) | 1.3 |

Table 7. *Hydrogen-bond interactions in the noncrystallographic dimer*

| Molecule *A* | | Molecule *B'* | | |
|---|---|---|---|---|
| Residue | Atom | Residue | Atom | Distance (Å) |
| 8Asn | N | 26Asp | O*D*2 | 3.3 |
| 8Asn | O | 54Asn | N*D*2 | 3.3 |
| 9Tyr | OH | 52Asp | O | 2.9 |
| 10Leu | N | 54Asn | O*D*1 | 3.1 |
| 24Ala | O | 161Ser | N | 2.8 |
| 26Asp | N | 159Asp | O | 2.9 |
| 26Asp | O*D*1 | 8Asn | N | 3.1 |
| 52Asp | O | 9Tyr | OH | 2.9 |
| 54Asn | N*D*2 | 8Asn | O | 3.2 |
| 54Asn | O*D*1 | 10Leu | N | 2.9 |
| 55Gln | N*E*2 | 279Asp | O*D*2 | 2.7 |
| 55Gln | N*E*2 | 278Asp | O*D*1 | 3.3 |
| 159Asp | O | 26Asp | N | 2.9 |
| 161Ser | N | 24Ala | O | 2.9 |
| 279Asp | O*D*2 | 55Gln | N*E*2 | 2.7 |

There is good electron density for the entire length of the two polypeptide chains except for the loop Glu239–Glu244. In particular, the loop region Pro292–Glu297 was found to have good electron density (Fig. 3) in contrast to the uncertain conformation observed in the orthorhombic complexes refined previously at higher resolutions (Abad-Zapatero, Rydel, Neidhart, Luly & Erickson, 1992). The weakest density in the present structure is associated with residues Asp278–Asp280.

The r.m.s. deviation between the 326 equivalent $C_\alpha$ pairs of the two liganded pepsin molecules is 0.34 Å (Table 8). Superposition of either of them on the structure of the unliganded pepsin (set 4PEP; Sielecki, Fedorov, Boodhoo, Andreeva & James, 1990) gives an r.m.s. deviation of approximately 0.84 Å for the complete chain (326 $C_\alpha$ pairs), or

Table 8. *Overall superposition between liganded and unliganded pepsin structures*

4PEP: native monoclinic pepsin (Sielecki, Fedorov, Boodhoo, Andreeva & James, 1990). PEP*A*: this crystal structure, molecule *A*. PEP*B*: this crystal structure, molecule *B*. 5PEP: pepsin/A63218 orthorhombic complex (Abad-Zapatero, Rydel, Neidhart, Luly & Erickson, 1992). The first row of each entry of the table is the root-mean-square deviation (Å) between the structures denoted by the corresponding row and column of the matrix. The integer number in the second row of each entry specifies the number of $C_\alpha$ pairs in the comparison as specified in (*a*), (*b*) and (*c*). (*a*) All the residues 1–326 for both. (*b*) Residues 1–199, 204–238, 245–249, 254–276, 282–289 and 298–326 for both. (*c*) Residues 1–277, 281–291 and 297–326 for both.

| | 4PEP | PEP*A* | PEP*B* | 5PEP |
|---|---|---|---|---|
| 4PEP | | 0.86 | 0.83 | 1.0 |
| | | 326[a] | 326[a] | 326[a] |
| PEP*A* | 0.57 | | 0.34 | 0.69 |
| | 299[b] | | 326[a] | 326[a] |
| PEP*B* | 0.53 | 0.31 | | 0.64 |
| | 299[b] | 299[b] | | 326[a] |
| 5PEP | 0.87 | 0.47 | 0.43 | |
| | 318[c] | 318[c] | 318[c] | |

0.55 Å for the 299 $C_\alpha$ pairs which were more accurately determined. Plots of the distances as a function of the residue number for pepsin *versus* pepsin/A62095 (Fig. 4*a*) and pepsin/A63218 *versus* pepsin/A62095 (Fig. 4*b*) reveal that certain portions of the polypeptide have moved significantly upon ligand binding.

A view of the present structure, and of the liganded pepsin found in the orthorhombic form, superposed on native porcine pepsin (set 4PEP) is presented in Fig. 5. As expected, the two liganded structures undergo similar conformational changes upon inhibitor binding. Nonetheless, these two structures also exhibit subtle differences, in spite of the close resemblance of the two inhibitors. The largest differences occur at the two short helices at the amino-end domain [helices $\alpha A$ (residues 48–52), $\alpha B$ (110–114); Abad-Zapatero, Rydel & Erickson, 1990], and in their vicinity. The inhibitors A63218 and A66702, which yielded the orthorhombic form, have the *p*-iodo substituent at the $P_3$ position (iodo-Phe). This residue has a considerably longer and bulkier side chain than leucine (present in A62095) and apparently pushed helix $\alpha B$ upward (Fig. 5), preventing it from adopting a conformation similar to that of native pepsin. This perturbation was accommodated by the neighboring residues in sheet (IV) [$\beta E3$ (70–74), $\beta F1$ (79–83), $\beta G3$ (105–106)] and by the nearby helix $\alpha A$ (48–52) in the pepsin structure. These alterations would explain the major differences observed in the vicinity of the active site between the enzymes in the two different complex forms (Figs. 4*b*, 5).

Apart from the ordering of the 292–297 segment, the largest differences in the carboxy-end domain occur at the most external loops of the flexible subdomain (Abad-Zapatero, Rydel & Erickson, 1990), particularly residues 239–255 and 278–281. The latter residues are probably very mobile in view of their weak electron density. On the other hand, residues 239–255 are well defined and their different conformation probably reflects local distortions due to crystal contacts.

*Pepsin–inhibitor interactions*

The electron density corresponding to the inhibitor A62095 was readily interpretable as an extended conformation (Fig. 6). This conformation has been found previously in many other inhibitors bound to a variety of aspartic proteinases (Bott, Subramanian

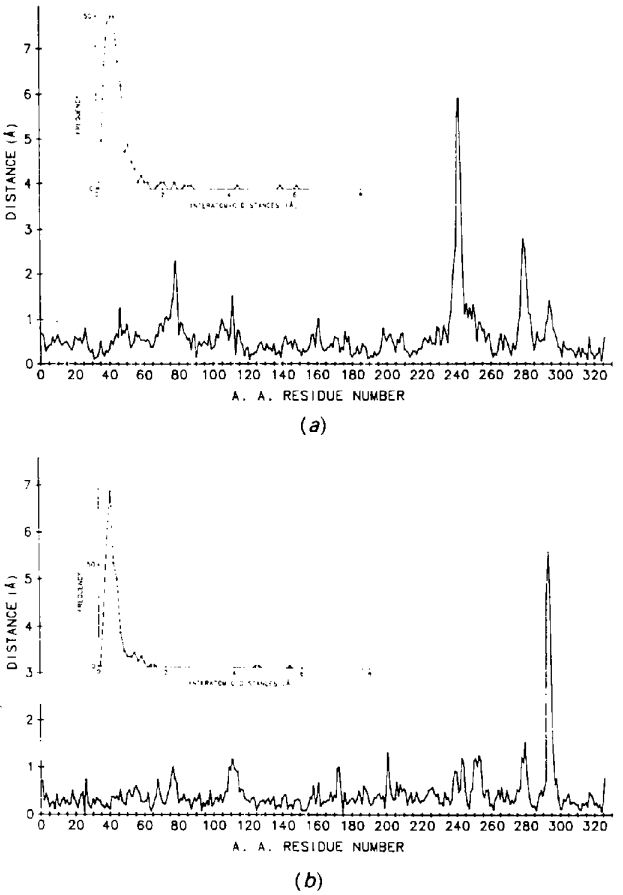


Fig. 4. Plot of the $C_\alpha$—$C_\alpha$ distance *versus* residue number between (*a*) the liganded and native pepsin after the overall least-squares superposition, (*b*) the orthorhombic (pepsin/A63218) and monoclinic (pepsin/A62095) complexes. The large distances in the 292–298 region in (*b*) are due to the uncertain conformation of this fragment in the orthorhombic form where it was considered to be disordered. Insets show the frequency distribution for the above distances.

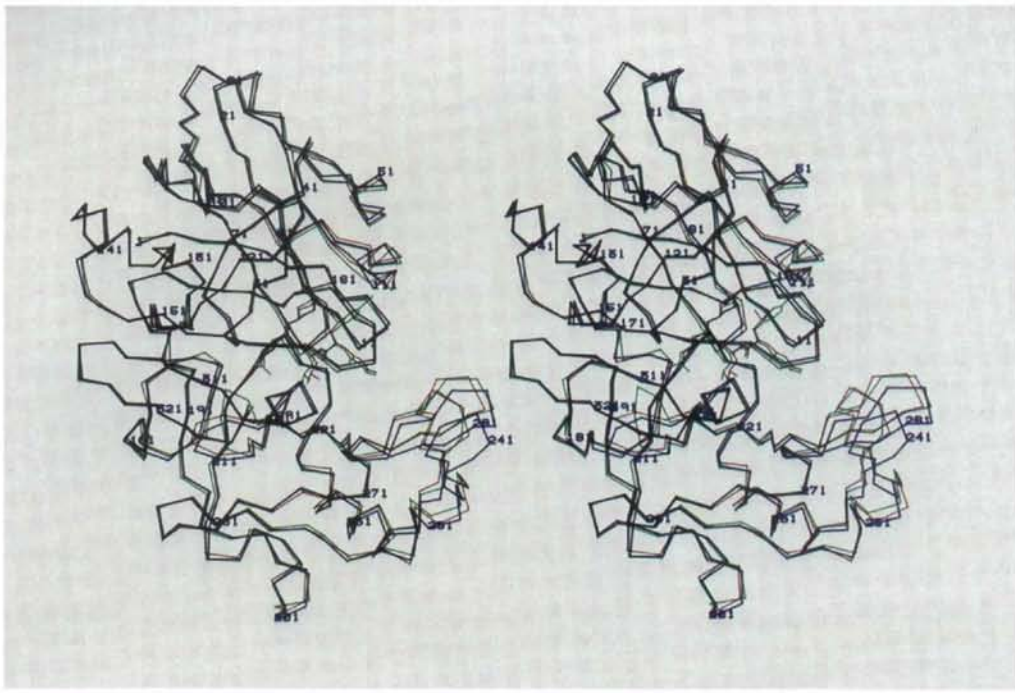

Fig. 5. Stereo diagram of the polypeptide backbone fold for native pepsin (blue) superposed with the polypeptide conformation of the enzyme observed in the orthorhombic (pepsin/A63218, green) and monoclinic (pepsin/A62095, red) complexes. The view emphasizes the inhibitor cavity and the regions of maximum displacement at the amino and carboxy domains.

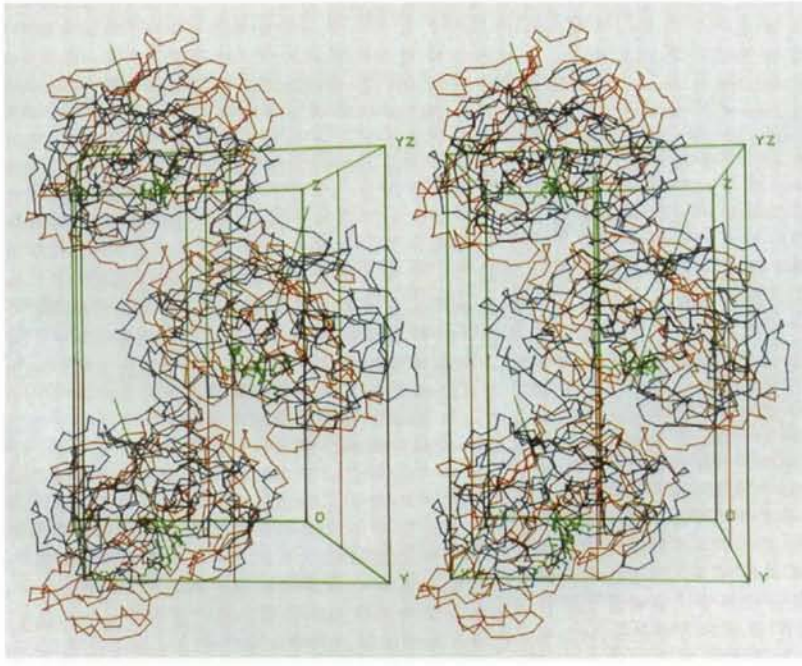


Fig. 9. Stereo diagram of the packing arrangement of the pepsin/A62095 complex molecules in the monoclinic crystal viewed along the crystallographic *b* axis (labeled *Y*). O denotes the origin of the unit cell. Molecules of the same color are generated by the crystallographic screw axes. The inhibitor molecules are also shown in contrasting colors. Pairs of molecules of different color illustrate the non-crystallographic dimer with the dyad (shown in green) passing in between two molecules, inclined 19.4° with respect to the crystallographic *c* axis (labeled *Z*). Boundaries of the unit cell are drawn in green and the location of the $2_1$ screw axes is indicated by green–red lines. The green–purple lines along the four vertical edges of the unit cell result from the superposition of the cell boundaries (green) and the green–red lines used for the screw axes. The program *TABLES* (Abad-Zapatero & O'Donnell, 1987) was used to prepare this diagram.

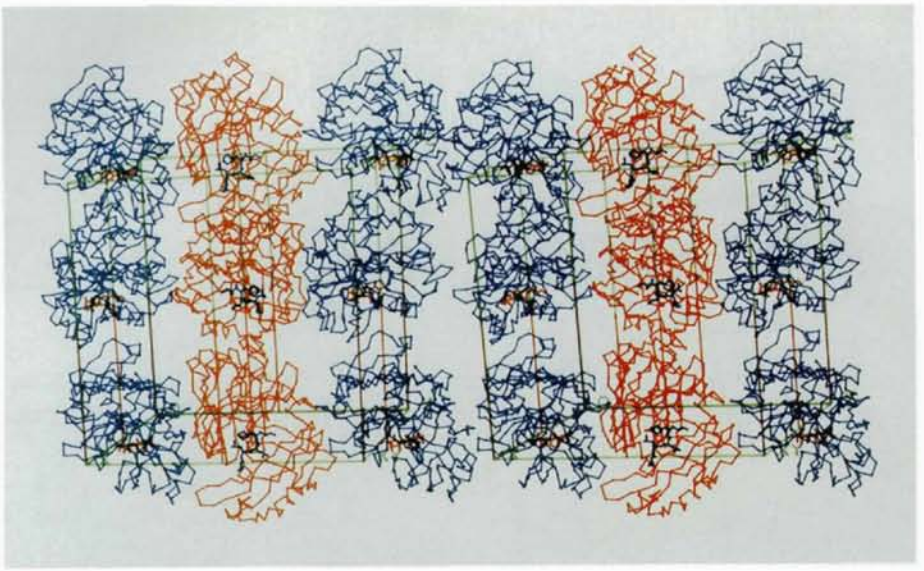

Fig. 10. Stereo diagram of the packing arrangement of the pepsin/A62095 complex molecules in the monoclinic crystal viewed along the *a* axis (labeled *X*). Colors and conventions as in Fig. 9.

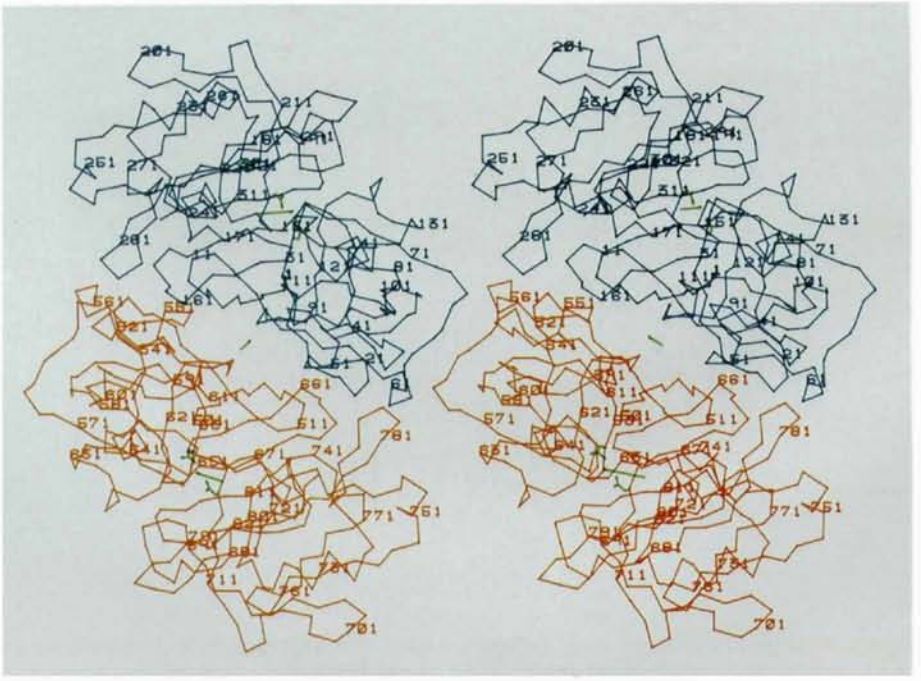

Fig. 11. Stereo diagram of the pepsin dimer found in the packing arrangement of pepsin molecules. The view is along the dimer axis shown in green (center). The interdomain dyads penetrate each molecule at the midpoint between the illustrated (in green) side chains of Asp32 and Asp215. They superpose approximately 70 residue pairs within each molecule, with an r.m.s. deviation of 2.4 Å. The angle between the dimer axis and the interdomain dyads is approximately 15°. Residue numbers for the second (red) molecule begin at 501.

& Davies, 1982; Suguna, Padlan, Smith, Carlson & Davies, 1987; Blundell, Cooper, Foundling, Jones, Atrash & Szelke, 1987; Foundling, Cooper, Watson, Cleasby, Pearl, Sibanda, Hemmings, Wood, Blundell, Valler, Norey, Kay, Boger, Dunn, Leckie, Jones, Atrash, Hallett & Szelke, 1987; Sali, Veerapandian, Cooper, Foundling, Hoover & Blundell, 1989; Veerapandian, Cooper, Sali & Blundell, 1990). The mode of binding and the specific hydrogen bonds to the protein molecule are very similar to the ones found in the pepsin/A66702 complex (Abad-Zapatero, Rydel, Neidhart, Luly & Erickson, 1992; Figs. 7, 8 and Table 9). Only two hydrogen bonds, mediated *via* water molecules, are absent in the present complex when compared to the orthorhombic one. One relating Thr74 to the $P1'$ hydroxyl of the glycol hook, and the second one from the $P_4$ carbonyl ($P_4$) to the carboxylic group of Glu287 (Fig. 8).

The number of non-bonded contacts ($< 4.1$ Å) between pepsin and the inhibitor is larger in the monoclinic than in orthorhombic form (35 *versus* 27; Abad-Zapatero, Rydel, Neidhart, Luly & Erickson, 1992) even though the ligand present in the latter (A66702) has more atoms (Table 1). This suggests a more intimate contact between the protein and the inhibitor in the complex found in the monoclinic crystal. We have recently determined the structure of another pepsin/renin inhibitor complex, in the same monclinic form, and refined it at 2.0 Å resolution. A detailed comparison among the different pepsin/renin inhibitor complex structures refined so far will be published elsewhere (Chen & Abad-Zapatero, 1992).

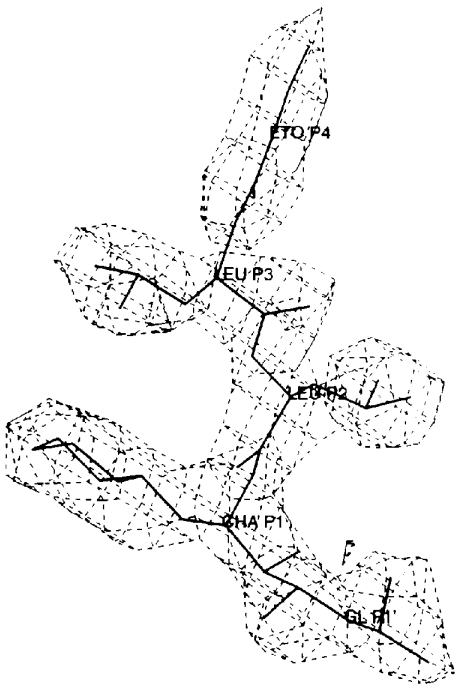


Fig. 6. View of the electron density corresponding to the inhibitor in the final $2F_o - F_c$ electron density map with the corresponding model for A62095. The contour level is $1\sigma$.

*Crystal packing*

The monoclinic crystals of the pepsin/A62095 complex exhibit a packing pattern (Figs. 9, 10) quite different from those of pepsinogen (Sielecki, Fujinaga, Read & James, 1991), native pepsin in either the monoclinic (Sielecki, Fedorov, Boodhoo, Andreeva & James, 1990; Abad-Zapatero, Rydel & Erickson, 1990) or hexagonal crystal forms (Cooper, Khan, Taylor, Tickle & Blundell, 1990), and the orthorhombic pepsin/inhibitor complexes (Abad-

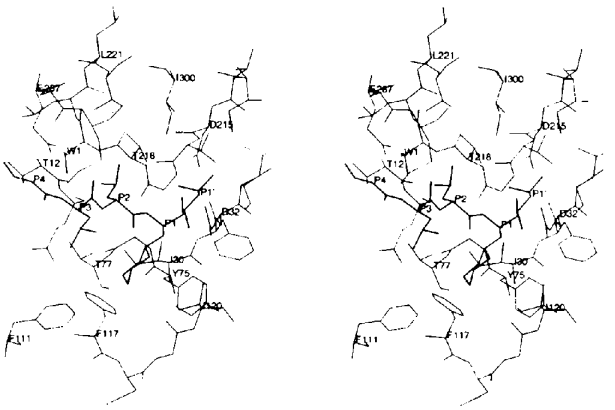

Fig. 7. Stereo diagram of the mode of binding of the A62095 inhibitor in the pepsin active site. The different subsites ($P_i$) of the inhibitor are indicated.

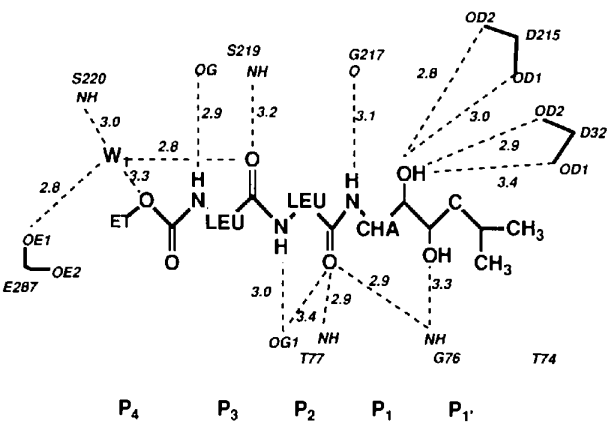


Fig. 8. Schematic representation of the hydrogen bonds formed between pepsin and the inhibitor A62095. The distances between acceptor and donor are given in Å averaged over the two independent molecules. $W_1$ denotes the approximate position of a tightly bound water molecule.

Table 9. *Residues lining the inhibitor binding subsites in the pepsin/A62095 complex*

Numbers in parentheses are distances from the amino-acid residue to the corresponding inhibitor subsite in Å. The first number refers to molecule *A*, the second to molecule *B*. – indicates no distances less than 4.1 Å.

| Inhibitor subsites | | | | |
|---|---|---|---|---|
| ETO | LEU | LEU | CHA | GL* |
| *P*4 | *P*3 | *P*2 | *P*1 | *P*1′ |
| Thr12(4.0, ) | Thr12( ,3.9) | Tyr75(4.1,3.7) | Ile30( ,3.8) | Gly34(3.6,3.5) |
| Thr77(4.1,4.1) | Glu13(4.0,3.9) | Gly76(3.0,2.8) | Asp32(2.9,2.8) | Thr75(3.6,3.4) |
| Ser219(3.4,3.6) | Ile30(–,4.0) | Thr77(2.8,2.9) | Gly34( ,3.9) | Gly76(3.4,3.2) |
| Leu220(3.9,4.0) | Thr77(3.9,3.7) | Gly217(3.9, ) | Tyr75(3.7,3.6) | Try189(3.9,3.5) |
| W1(3.3,3.2) | Phe111( ,3.5) | Thr218(3.5,3.9) | Thr77(3.0,3.0) | Ile213(3.6,3.5) |
| | Phe117(–,3.9) | Thr222( ,3.8) | Phe111(–,3.5) | Asp215(3.4,3.5) |
| | Gly217(3.6,3.7) | Glu287(4.0,3.9) | Phe117(3.7,3.7) | Ile300(3.7,3.7) |
| | Thr218(3.3,3.4) | Met289(3.5,3.4) | Ile120(3.6,4.0) | |
| | Ser219(2.8,2.9) | Ile300(3.8, ) | Asp215(2.7,2.8) | |
| | W1(2.7,2.9) | | Gly217(3.0,3.2) | |
| | | | Thr218(3.4,3.9) | |
| *S*4 | *S*3 | *S*2 | *S*1 | *S*1′ |
| Pepsin subsites | | | | |

*GL denotes the *P*1′ subsite of the alkyl-diol inhibitor (Fig. 7).

Zapatero, Rydel, Neidhart, Luly & Erickson, 1992). The crystallization conditions, the presence of the pro-peptide in the zymogen, and also the type of inhibitor, are all variables that influence the crystal packing.

Monoclinic crystals of native pepsin were grown by slight variation of the batch procedure originally described by Northrop (1946) using ethanol as the precipitant in acidic (pH = 2.0) conditions (Abad-Zapatero, Rydel & Erickson, 1990; Sielecki, Fedorov, Boodhoo, Andreeva & James, 1990). The first protein crystals ever to be examined by X-rays were of a hexagonal form of pepsin (Bernal & Crowfoot, 1934). These crystals have been grown recently by slowly cooling a highly concentrated (280 mg ml $^{-1}$) pepsin solution at pH 3.6, and the corresponding structure determined and refined at 2.3 Å resolution (Cooper, Khan, Taylor, Tickle & Blundell, 1990). Both the monoclinic and the hexagonal forms have a single pepsin molecule in the asymmetric unit. Crystals of pepsinogen (monoclinic, *C*2) were grown at pH 6.1 by the hanging-drop method using $Li_2SO_4$ as precipitating agent (Sielecki, Fujinaga, Read & James, 1991). An orthorhombic form of pepsin was obtained upon co-crystallization in the presence of inhibitors containing *p*-iodophenylalanine at the $P_3$ under conditions similar to those that produced the native monoclinic form (Abad-Zapatero, Rydel, Neidhart, Luly & Erickson, 1992). The monclinic form described in this paper, with two molecules in the asymmetric unit, was obtained under the same conditions as the orthorhombic form with chemically similar inhibitors, containing either phenylalanine (A61963) or leucine (A62095) (Fig. 1, Table 1). Apparently, the presence of iodine in the *para* position of the phenylalanine ring at position $P_3$ has a major influence in the crystal packing.

The two independent molecules (*A* and *B*) found in the structure solution are related by rotation of 38.7° about an axis parallel to the crystallographic *b* axis. The distance between their centers of mass is approximately 50 Å and the molecules do not interact. However, molecule *B*′ (related to *B* by the crystal screw axis) is in intimate contact with molecule *A* (approximately 1100 Å$^2$ of surface contact; Kabsch & Sander, 1983), forming a noncrystallographic dimer (Figs. 9, 10). The noncrystallographic dyad ($\kappa$ = 180.0°) lies in the plane perpendicular to the crystal *b* axis and is inclined 19.4° from the crystallographic $2_1$ axis (Fig. 2*b*). This dyad is located between the interdomain axes of the two pepsin molecules. Each intramolecular dyad pierces the corresponding pepsin molecule at the midpoint between Asp32 and Asp215, and intersects the interdomain sheet halfway between residues Phe151 and Thr311. The average angle between the dimer axis and the interdomain dyads is approximately 15° (Fig. 11).

Viewed along the *b* axis, the crystal packing consists of noncrystallographic dimers, with their axes inclined alternately on both sides of the crystallographic *c* axis (Fig. 9). Viewed down the *a* axis, the crystal is made up of columns of pepsin molecules interacting along the crystallographic screw axes of the cell with the side contacts being provided by the noncrystallographic symmetry (Fig. 10).

Each of the two molecules forming these dimers makes a total of approximately 400 direct contacts with protein atoms of seven neighboring molecules (< 4.1 Å) (Table 10*c*, Fig. 9). This number does not include the solvent-mediated hydrogen-bonding interactions that exist at the molecular interfaces. The largest number of contacts (214, 53%) are between the two molecules which form the noncrystallographic dimer. This contact area consists pre-

Table 10. *Intermolecular contacts in crystals of native and liganded pepsin*

| Residues at the interface: Molecule at $x, y, z$ | Residues at the interface: Transformed molecule | Transformation operator | No. of contacts $< 4.1$ Å (%) |
|---|---|---|---|
| (*a*) Native pepsin[a] | | | |
| 70 74, 127, 130 131, 290 | 7, 158 162, 253, 326 | (*A*) $x, y-1, z$ shortest axis translation | 62 (27) |
| 74 79, 108 111, 114, 241 243, 245, 286 287 | 158, 236, 238 241, 246 248, 251, 254, 277 281 | (*B*) $-x, y-\frac{1}{2}, -z$ $2_1$ axis | 92 (39) |
| 17, 23 24, 26, 60 | 44, 59, 68, 105 | (*C*) $-x, y-\frac{1}{2}, -z+1$ $2_1$ axis | 21 (10) |
| 199 202, 259, 266 | 193, 195, 207 211, 295 | (*D*) $-x+1, y+\frac{1}{2}, -z$ $2_1$ axis | 29 (12) |
| 1, 147 148, 169 172, 193, 195, 207 211, 295 | 141 145 | (*E*) $-x+1, y-\frac{1}{2}, -z+1$ $2_1$ axis | 29 (12) |
| (*b*) Pepsin/A63218[b] | | | |
| 70 74, 126 127, 130 131, 290, 293, 297 | 7, 158 162, 253, 272 | (*A*) $x, y, z-1$ shortest axis translation | 81 (31) |
| 59, 61 65, 83, 105 | 109 111, 114, 240 242 | (*B*) $x, y-\frac{1}{2}, -z+\frac{1}{2}$ $2_1$ axis | 84 (32) |
| 24 27, 51 52, 54 55 | 248 250, 279 280 | (*C*) $-x, y+\frac{1}{2}, -z+\frac{1}{2}$ $2_1$ axis | 33 (12) |
| 200 202, 251, 259, 266 | 193, 207 211 | (*D*) $x+\frac{1}{2}, -y, z+\frac{1}{2}$ $2_1$ axis | 30 (11) |
| 170 173, 175, 177 179 | 141 144 | (*E*) $-x+\frac{1}{2}, -y+1, z+\frac{1}{2}$ $2_1$ axis | 36 (14) |
| (*c*) Pepsin/A62095[c] | | | |
| Molecule *A* at $x, y, z$ | Transformed molecule *B'* | | |
| 7 10, 17, 24 26, 43, 45, 52 55, 60, 114, 158 161, 278 279 | 7–10, 19, 23 27, 43, 51 55, 60,114,158 161, 278 279 | (*A*) $x, y, z$ on *B'* (noncrystallographic dimer) | 214 (53) |
| 185 186, 193, 208 209, 211, 294 296 | 185 186, 209 211, 294 296 | (*B*) $x, y-1, z$ on *B'* | 48 (12) |
| 1 | 202 | (*C*) $x+2, y+1, z+\frac{1}{2}$ on *B'* | 3 (1) |
| Molecule *A* at $x, y, z$ | Transformed molecule *A* | | |
| 65 67, 69, 132, 134 | 248, 250, 279 280 | (*D*) $x+1, y, z$ on *A* | 26 (6) |
| 172 173, 178 179, 181 | 225 226, 229, 239 243 | (*E*) $-x+1, -y, z+\frac{1}{2}$ on *A* | 38 (9) |
| Molecule *B'* at $x, y, z$ | Transformed molecule *B'* | | |
| 62 63, 65 67, 69, 86, 141 142, 144 | 108 110, 225, 239, 241 242, 290 | (*F*) $-x+1, y+1, z+\frac{1}{2}$ on *B'* | 39 (10) |
| 1, 3, 171 173, 175 | 246, 248 250, 280 281 | (*G*) $x+2, y+1, z+\frac{1}{2}$ on *B'* | 36 (9) |

Notes: (*a*) Calculated using the Protein Data Bank set 4PEP (Sielecki, Fedorov, Boodhoo, Andreeva & James, 1990). (*b*) From the structure of the pepsin/A63218 complex (Abad-Zapatero, Rydel, Neidhart, Luly & Erickson, 1992). (*c*) This work.

dominantly of polar residues within the amino-terminal domain (Table 7), with about one third of the interactions involving residues 52–55. Preliminary fluorescence polarization data of a pepsin solution (pH = 2.0), in the presence of A62095 and 20% ethanol, suggest that a dimer is present prior to crystallization (Matayoshi & Abad-Zapatero, unpublished observations). Therefore, it is probable that the noncrystallographic dimer is the initial building unit of the crystal. Such a building unit has not been found in any of the crystal packings of related pepsin structures.

The crystal contacts along the shortest axis translation are preserved between the monoclinic native pepsin and the orthorhombic complex form (operator *A*, Table 10*a*,*b*), resulting in very similar cell constants for the shortest cell spacing of these two crystal forms (Table 1). However, the binding of the inhibitor disturbs the conformation of several contact surfaces (residues 40–60, 70–80, 100–115, 235–245 and 275–285, Fig. 4*a*), and only two of the four remaining crystal contacts are partially maintained between them (operators *D*, *E*, Table 10).

In the pepsin/A62095 complex, the absence of a bulky substituent at the $P_3$ position allows a closer interaction between the enzyme and the inhibitor (Fig. 5), and affects predominantly the contact areas near the $P_3$ position (residues 70–80, 105–120) (Fig. 4*b*). Surprisingly, this small alteration disrupts the numerous contacts which preserved the shortest cell axis (residues 70–74, operator *A*, Table 10) and a different crystal form is observed. In fact, these residues do not participate in any crystal contacts in the liganded monoclinic form, and only one interface is partially maintained between the two complex crystals (operator *B* in Table 10*b* and *F* in Table 10*c*).

We thank Dr J. Greer for critical reading of the manuscript and for support during the course of this project. We appreciate the assistance of Pat Collins with the artwork and Mark Stearns, Dick Hale and Art Noel (Corporate Media Services) with the preparation of the illustrations. The constructive criticisms of the anonymous referees are appreciated.

## References

ABAD-ZAPATERO, C. & O'DONNELL, T. J. (1987). *J. Appl. Cryst.* **20**, 532–535.

ABAD-ZAPATERO, C., RYDEL, T. J. & ERICKSON, J. W. (1990). *Proteins Struct. Funct. Genet.* **8**, 62–81.

ABAD-ZAPATERO, C., RYDEL, T. J., NEIDHART, D., LULY, J. & ERICKSON, J. W. (1992). *Structure and Function of the Aspartic Proteinases: Genetics, Structures and Mechanisms. Advances in Experimental Medicine and Biology*, Vol. 306, edited by B. M. DUNN, pp. 9–21. New York: Plenum Press.

ANDREEVA, N. S., FEDOROV, A. A., GUSTCHINA, A. E., RISKULOV, R. R., SAFRO, M. G. & SHUTZKEVER, N. E. (1978). *Mol. Biol. (Engl. Transl.)*, **12**, 704–707.

ANDREEVA, N. S. & GUSTCHINA, A. E. (1979). *Biochem. Biophys. Res. Commun.* **87**, 32–42.

ANDREEVA, N. S., ZDANOV, A. S., GUSTCHINA, A. E. & FEDOROV, A. A. (1984). *J. Biol. Chem.* **259**, 11353–11365.
BERNAL, J. D. & CROWFOOT, D. (1934). *Nature (London)*, **133**, 794–795.
BLUNDELL, T., COOPER, J. B., FOUNDLING, S. I., JONES, D. M., ATRASH, B. & SZELKE, M. (1987). *Biochemistry*, **26**, 5585 5590.
BLUNDELL, T., JENKINS, J., PEARL, L., SEWELL, T. J., COOPER, J. B., TICKLE, I. J., VEERAPANDIAN, B. & WOOD, S. P. (1990). *J. Mol Biol.* **211**, 919 941.
BLUNDELL, T. L., SEWELL, B. T. & MCLACHLAN, A. D. (1979). *Biochim. Biophys. Acta*, **580**, 24–31.
BOLIS, G. & GREER, J. (1989). *Computer-Aided Drug Design. Methods and Applications*, edited by T. J. PERUN & C. L. PROPST, pp. 297–326. New York: Dekker.
BOTT, R., SUBRAMANIAN, E. & DAVIES, D. R. (1982). *Biochemistry*, **21**, 6956–6962.
BRÜNGER, A. T., KARPLUS, M. & PETSKO, G. A. (1989). *Acta Cryst.* A**45**, 50 61.
CHEN, L. & ABAD-ZAPATERO, C. (1992). In preparation.
COOPER, J. B., KHAN, G., TAYLOR, G., TICKLE, I. J. & BLUNDELL, T. L. (1990). *J. Mol. Biol.* **214**, 199 222.
CRAVEN, B. M. (1975). *ROTRAN*. Univ. of Pittsburgh, USA.
CROWTHER, R. A. & BLOW, D. W. (1967). *Acta Cryst.* **23**, 544–548.
CYGLER, M. & ANDERSON, W. F. (1988*a*). *Acta Cryst.* A**44**, 38–45.
CYGLER, M. & ANDERSON, W. F. (1988*b*). *Acta Cryst.* A**44**, 300 308.
DAVIES, D. R. (1990). *Annu. Rev. Biophys. Biophys. Chem.* **19**, 189 215.
FITZGERALD, P. M. D. (1988). *J. Appl. Cryst.* **21**, 273 278.
FOUNDLING, S. I., COOPER, J., WATSON, F. E., CLEASBY, A., PEARL, L. H., SIBANDA, B. L., HEMMINGS, A., WOOD, S. P., BLUNDELL, T. L., VALLER, M. J., NOREY, C. G., KAY, J., BOGER, J., DUNN, B. M., LECKIE, B. J., JONES, D. M., ATRASH, B., HALLETT, A. & SZELKE, M. (1987). *Nature (London)*, **327**, 349–352.
HSU, I., DELBAERE, L. T. J., JAMES, M. N. G. & HOFMANN, T. (1977). *Nature (London)*, **266**, 140–145.
HUTCHINS, C. & GREER, J. (1991). *Crit. Rev. Biochem. Mol. Biol.* **26**, 77 127.
JAMES, M. N. G. & SIELECKI, A. R. (1983). *J. Mol. Biol.* **163**, 299–361.
KABSCH, W. & SANDER, C. (1983). *Biopolymers*, **22**, 2577 2637.
KOSTKA, V. (1985). Editor. *Aspartic Proteinases and Their Inhibitors*, Proceedings of the FEBS Advanced Course No. 84/07, Prague, Czechoslovakia. New York: Walter de Gruyter.
LATTMAN, E. E. & LOVE, W. E. (1972). *Acta Cryst.* B**26**, 1854 1857.
MILLER, M., JASKOLSKI, M., RAO, J. K. M., LEIS, J. & WLODAWER, A. (1989). *Nature (London)*, **337**, 576–579.
Molecular Structure Corporation (1989). *TEXSAN. Single Crystal Structure Determination Software*. Version 5.0. MSC, The Woodlands, Texas, USA.
NAVIA, M. A., FITZGERALD, P. M. D., MCKEEVER, B. M., LEU, C.-T., HEIMBACH, J. C., HERBER, W. K., SIGAL, I. S., DARKE, P. L. & SPRINGER, J. P. (1989). *Nature (London)*, **337**, 615 620.
NORTHROP, J. H. (1946). *J. Gen. Physiol.* **30**, 177–184.
RAO, G. K. M., ERICKSON, J. W. & WLODAWER, A. (1991). *Biochemistry*, **30**, 4663 4671.
ROSSMANN, M. G. (1972). Editor. *The Molecular Replacement Method*. New York: Gordon and Breach.
RÜCHEL, R. (1981). *Biochim. Biophys. Acta*, **659**, 99 113.
SALI, A., VEERAPANDIAN, B., COOPER, J. B., FOUNDLING, S. I., HOOVER, D. J. & BLUNDELL, T. L. (1989). *EMBO J.* **8**, 2179–2188.
SHAM, H. L., BOLIS, G., STEIN, H. H., FESIK, S. W., MARCOTTE, P. A., PLATTNER, J. J., REMPEL, C. A. & GREER, J. (1988). *J. Med. Chem.* **31**, 289 295.
SHERIFF, S., PADLAND, E. A., COHEN, G. H. & DAVIES, D. R. (1990). *Acta Cryst.* B**46**, 418 425.
SIELECKI, A. R., FEDOROV, A. A., BOODHOO, A., ANDREEVA, N. S. & JAMES, M. N. G. (1990). *J. Mol. Biol.* **214**, 143 170.
SIELECKI, A. R., FUJINAGA, M., READ, R. J. & JAMES, M. N. G. (1991). *J. Mol. Biol.* **49**, 671 692.
STEIGEMANN, W. (1974). PhD Thesis. Technische Univ., München, Germany.
SUGUNA, K., BOTT, R. R., PADLAN, E. A., SUBRAMANIAN, E., SHERIFF, S., COHEN, G. H. & DAVIES, D. R. (1987). *J. Mol. Biol.* **196**, 877–900.
SUGUNA, K., PADLAN, E. A., SMITH, C. W., CARLSON, W. D. & DAVIES, D. R. (1987). *Proc. Natl Acad. Sci. USA*, **84**, 7009–7013.
TANG, J., JAMES, M. N. G., HSU, I. N., JENKINS, J. A. & BLUNDELL, T. L. (1978). *Nature (London)*, **271**, 618 621.
VEERAPANDIAN, B., COOPER, J. B., SALI, A. & BLUNDELL, T. L. (1990). *J. Mol. Biol.* **216**, 1017 1029.
WLODAWER, A., MILLER, M., JASKOLSKI, M., SATHYANARAYANA, B. K., BALDWIN, E. T., WEBER, I. T., SELK, L. M., CLAWSON, L., SCHNEIDER, J. & KENT, S. B. H. (1989). *Science*, **245**, 616–621.

*Acta Cryst.* (1992). B**48**, 488–492

# Crystal and Molecular Structures of Propanediamine Complexed with L- and DL-Glutamic Acid: Effect of Chirality on Propanediamine

BY S. RAMASWAMY AND M. R. N. MURTHY

*Molecular Biophysics Unit, Indian Institute of Science, Bangalore* 560012, *India*

(*Received* 6 *August* 1991; *accepted* 13 *January* 1992)

## Abstract

The structures of complexes of 1,3-diaminopropane with L- and DL-glutamic acid have been determined. L-Glutamic acid complex: $C_3H_{12}N_2^{2+}.2C_5H_8NO_4^-$, $M_r = 368.4$, orthorhombic, $P2_12_12_1$, $a = 5.199$ (1), $b = 16.832$ (1), $c = 20.076$ (3) Å, $V = 1756.6$ (4) Å$^3$, $Z = 4$, $D_x = 1.39$ g cm$^{-3}$, $\lambda$(Mo $K\alpha$) = 0.7107 Å, $\mu = 1.1$ cm$^{-1}$, $F(000) = 792$, $T = 296$ K, $R = 0.044$ for 1276 observed reflections. DL-Glutamic acid com-

0108-7681/92/040488-05$06.00 